EFFECT OF B, Si AND P CO-DOPING ON ELECTRONIC PROPERTIES OF Mn-DOPED AlN CRYSTALS

S.V. SYROTYUK, V.M. SHVED

Lviv Polytechnic National University, Semiconductor Electronics Department
(12, Bandera Str., Lviv 79000, Ukraine)

PACS 71.20.-b, 71.10.-w
©2011

The partial and total electron state densities of Mn-doped AlN crystals co-doped with B, Si, and P atoms are calculated for the up and down orientations of the spin moment. The comparison of the electron state densities of pure and Mn-doped AlN crystals shows that the Mn impurity leads to the appearance of hybridized energy states with *p*- and *d*-symmetry in the forbidden band. The co-doping with B, Si, and P atoms results in a change of the electron state density and the spin magnetic moments on all atoms of the crystal.

1. Introduction

Nitrides of elements of the third group with admixtures of transition metals are in the focus of attention of investigators due to their possible use in high-power and high-frequency transistors, photodiodes emitting in the blue and ultraviolet spectral regions, laser diodes, and so on [1]. These materials are considered as promising for the use in spintronics [1,2]. In this case, a significant role is played by the magnetic moment appearing due to the presence of a transition metal admixture. For optoelectronics, it is important to know the energy band structure that is cardinally changed in the spectral range of practical interest after the introduction of a transition metal impurity. The electron state densities of AlN crystals with admixtures of transition metals have been recently calculated with the help of the pseudopotential method [3]. We applied the Green's function technique to calculate the electron state densities of Mn-doped AlN crystals co-doped with B, Si, and P elements with regard for two vacancies in the unit cell [4–7].

The aims of this work were as follows: 1) to calculate the electron state densities of a Mn-doped AlN crystal; 2) to perform calculations in the case of additional doping with B, Si, and P elements; 3) to calculate the Fermi energies, electron state densities at the Fermi level, and spin magnetic moments on atoms and vacancies.

Section 2 briefly describes the Green's function formalism. In Section 3, we report the results of calculating the electron state densities of doped AlN crystals.

2. Green Function Method

The electron energy spectrum is derived from the Schrödinger equation

$$(\nabla^2/2 + E(\mathbf{k}))\Psi_{\mathbf{k}}(\mathbf{r}) = V(\mathbf{r})\Psi_{\mathbf{k}}(\mathbf{r}), \tag{1}$$

where V stands for the potential of a crystal, $\Psi_{\mathbf{k}}$ and $E_{\mathbf{k}}$ is the eigenvector and the eigenvalue of an electron at a point $\mathbf{k}$ of the first Brillouin zone, respectively.

The unknown wave function in the crystal entering Eq.(1) can be found as a solution of the integral equation [4]

$$\Psi_{\mathbf{k}}(\mathbf{r}) = \int d\mathbf{r}' V(\mathbf{r}') G_{\mathbf{k}}(\mathbf{r}-\mathbf{r}')\Psi_{\mathbf{k}}(\mathbf{r}'), \tag{2}$$

where the Green's function of a free electron is determined in terms of its energy spectrum $E^0_{n,\mathbf{k}}$

$$G_{\mathbf{k}}(\mathbf{r},\mathbf{r}') = 1/\Omega \sum_n \frac{\exp(i\mathbf{k}_n(\mathbf{r}-\mathbf{r}'))}{E(\mathbf{k}) - E^0_{n,\mathbf{k}}}. \tag{3}$$

The Korringa–Kohn–Rostoker (KKR) theory is considerably simplified if

$$V(\mathbf{r}) = \begin{cases} V(|\mathbf{r}|), & r < r_{MT}, \\ 0, & r > r_{MT}. \end{cases} \tag{4}$$

which yields the system of linear homogeneous equations

$$\sum_{l'm'} \mathrm{M}_{lm;l'm'}(\mathbf{k}) c_{l'm'}(\mathbf{k}) = 0. \tag{5}$$

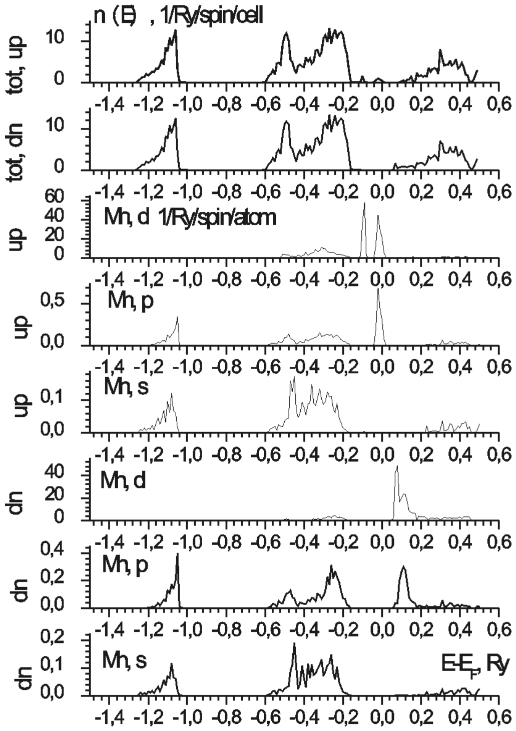

Fig. 1. Total and partial electron state densities in the Mn-doped (1%) AlN crystal

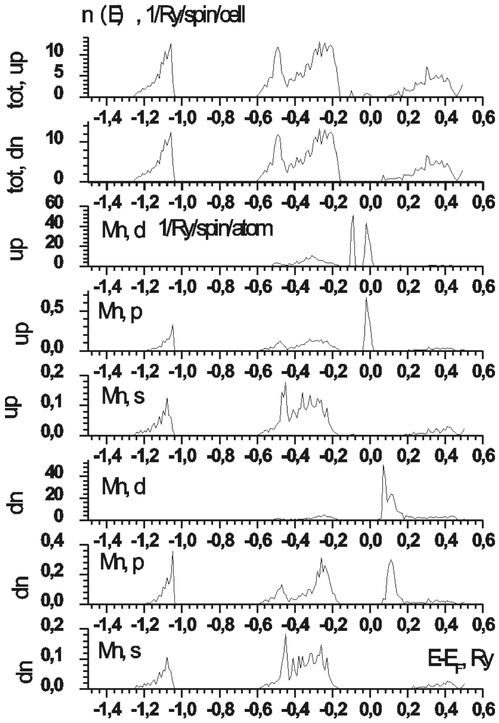

Fig. 2. The same as in Fig.1 for the Mn-doped (1%) AlN crystal co-doped with B (1%)

Calculating the energy eigenvalues and eigenvectors from system (5), one obtains the electron state density [4-7]:

$$n(E) = -1/\pi \int d\mathbf{r} G(\mathbf{r}, \mathbf{r}, E). \tag{6}$$

The calculations were performed using the KKR–LSDA (local spin density approximation) technique proposed in [6,7]. The relativistic effects were taken into account with the help of the scalar relativistic approximation. The integration over the quasiwave vector in the irreducible part of the Brillouin zone was carried our using a 10×10×10 array of dots.

3. Results and Discussion

We calculated the electronic properties of doped AlN crystals. The obtained results are presented in Figs. 1–8 and Table. The notations "*dn*" and "*up*" correspond to "down-spin" and "up-spin", respectively. In Fig. 1, one can see the partial densities of down-spin (curves *1–3* from below) and up-spin (curves *4–6* from below) electron states. Curves *7* and *8* demonstrate the total (*tot*) down-spin and up-spin electron state densities, respectively. The notations in all the figures are the same.

One can see from Fig. 1 that, in the forbidden band, there appear four groups of hybridized states with *p*- and *d*-symmetry that were absent in pure aluminum nitride. The Fermi level is located at the center of the forbidden band and is chosen as the energy reference. The *p*- and *d*-symmetry states caused by the presence of the Mn impurity are localized below the Fermi level (up-spin) and above it (down-spin). As is shown in Table, the electron state densities at the Fermi level in the $\mathrm{Al}_{0.99}\mathrm{Mn}_{0.01}\mathrm{N}$ crystal are different, i.e. the Mn substitutional impurity (1%) results in the significant spin polarization of the electron density. The spin magnetic moments on the Al and N atoms, as well as those of vacancies, are small though non-zero, in contrast to pure AlN. The largest magnetic spin moment is certainly observed on the Mn atom.

It is worth paying attention to the considerable difference between the curves of the partial densities of Mn states with *p*- and *d*-symmetry corresponding to the opposite spin orientations and localized from the both sides of the Fermi level. This difference directly testifies to the existence of the non-zero magnetic moment in the crystal.

The data presented in Figs. 2–4 and Table allow one to trace the variation of the electron state density under

Electronic and magnetic properties of $Al_{1-x-y}Mn_xX_yN$, $X = (B, Si, P)$ crystals. Here, ε_F is the Fermi energy (Ry), "up" and "dn" stand for "up-spin" and "down-spin", respectively, $n(\varepsilon_F)$ is the electron state density at the Fermi level (1 / Ry / spin / cell), and μ_s is the spin moment (μ_B). The coordinates of vacancy 1 and vacancy 2 are $a(1/2;1/2;1/2)$ and a (3/4; 3/4; 3/4), respectively, a =4.36 Å

	$Al_{0.99}Mn_{0.01}N$	$Al_{0.98}Mn_{0.01}B_{0.01}N$	$Al_{0.98}Mn_{0.01}Si_{0.01}N$	$Al_{0.98}Mn_{0.01}P_{0.01}N$
ε_F. up	0.9666	0.9650	1.0465	1.0559
ε_F. dn	0.9654	0.9637	1.0451	1.0547
$n(\varepsilon_F)$. up	0.7493	0.7510	0.0305	0.5052
$n(\varepsilon_F)$. dn	0.0236	0.0229	0.0627	0.8013
μ_S on Al	0.0006	0.0006	0.0007	0.0006
μ_S on Mn	3.0498	3.0493	3.2859	3.2191
μ_S on		0.0018(B)	0.0017(Si)	−0.0632(P)
μ_S on N	0.0038	0.0038	0.0048	0.0029
μ_S on vac. 1	0.0004	0.0004	0.0005	0.0003
μ_S on vac. 2	0.0038	0.0028	0.0038	0.0031
	$Al_{0.98}Mn_{0.02}N$	$Al_{0.97}Mn_{0.02}B_{0.01}N$	$Al_{0.97}Mn_{0.02}Si_{0.01}N$	$Al_{0.97}Mn_{0.02}P_{0.01}N$
ε_F, up	1.0032	1.0018	1.0236	1.0364
ε_F, dn	1.0032	1.0018	1.0236	1.0336
$n(\varepsilon_F)$, up	0.4485	0.4449	08326	0.0419
$n(\varepsilon_F)$, dn	0.4485	0.4449	0.8321	0.2856
μ_S on Al	0.0000	0.0000	0.0000	0.0013
μ_S on Mn	0.0000	0.0000	0.0003	3.2804
μ_S on		0.0000(B)	0.0000(Si)	0.0066(P)
μ_S on N	0.0000	0.0000	0.0000	0.0095
μ_S on vac. 1	0.0000	0.0000	0.0000	0.0011
μ_S on vac. 2	0.0000	0.0000	0.0000	0.0075

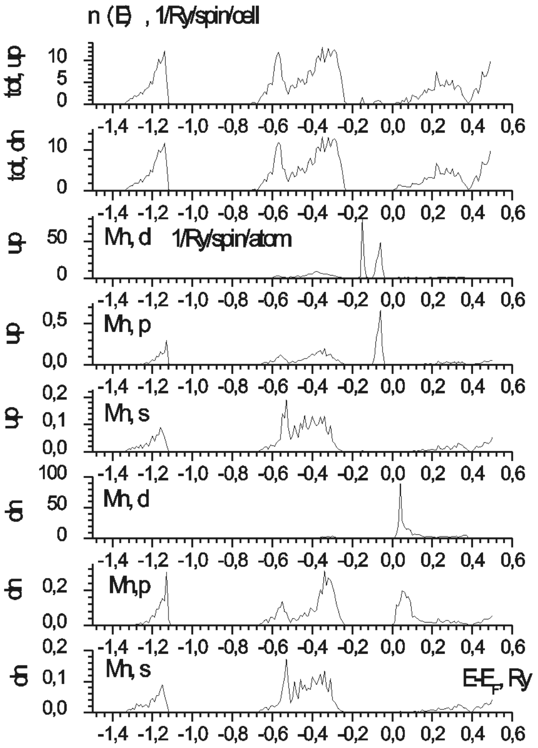

Fig. 3. The same as in Fig.1 for the Mn-doped (1%) AlN crystal co-doped with Si (1%)

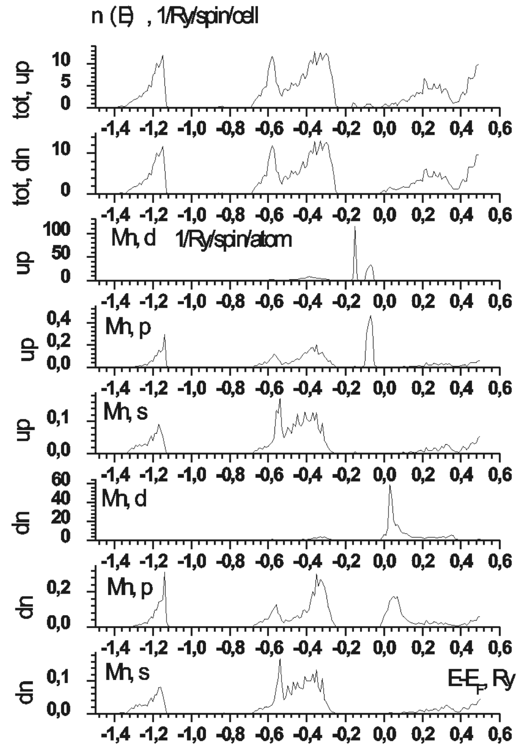

Fig. 4. The same as in Fig.1 for the Mn-doped (1%) AlN crystal co-doped with P (1%)

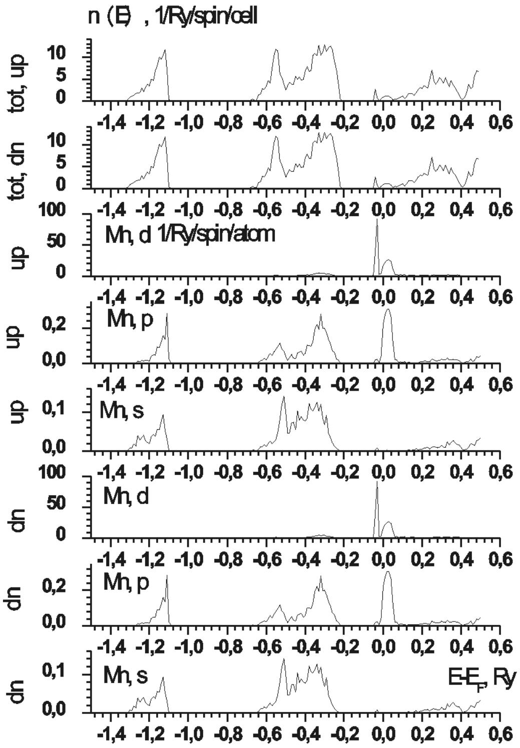

Fig. 5. The same as in Fig.1 for the Mn-doped (2%) AlN crystal co-doped with Si (1%)

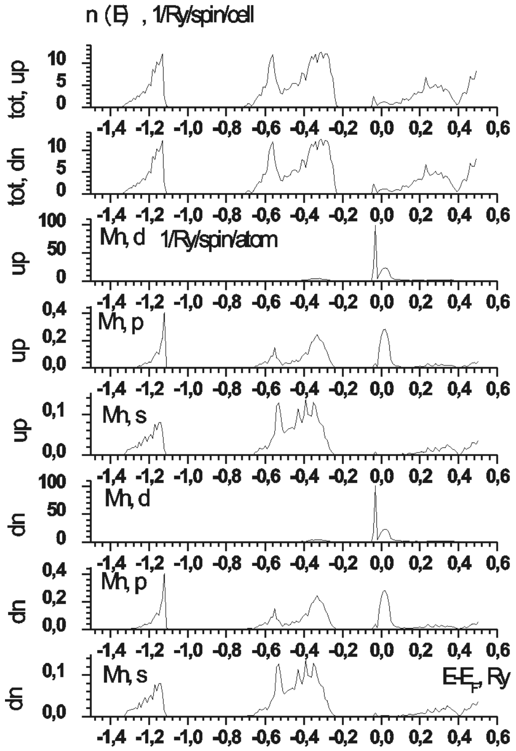

Fig. 6. The same as in Fig.1 for the Mn-doped (1%) AlN crystal co-doped with Si (2%)

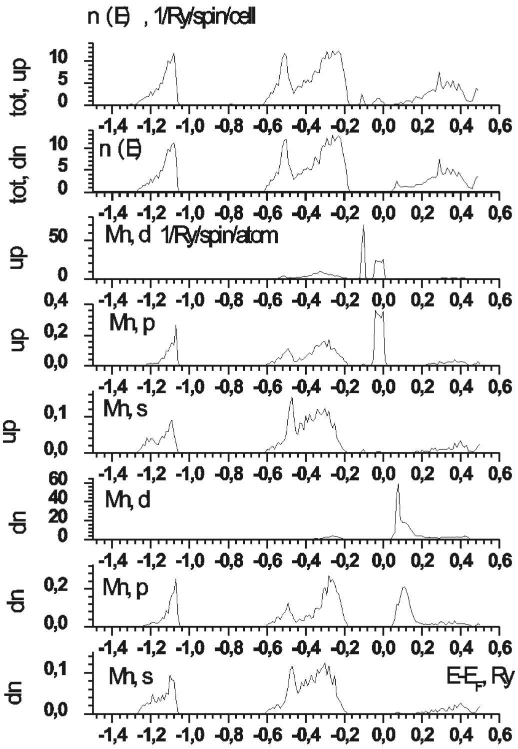

Fig. 7. The same as in Fig.1 for the Mn-doped (2%) AlN crystal co-doped with P (0.5%)

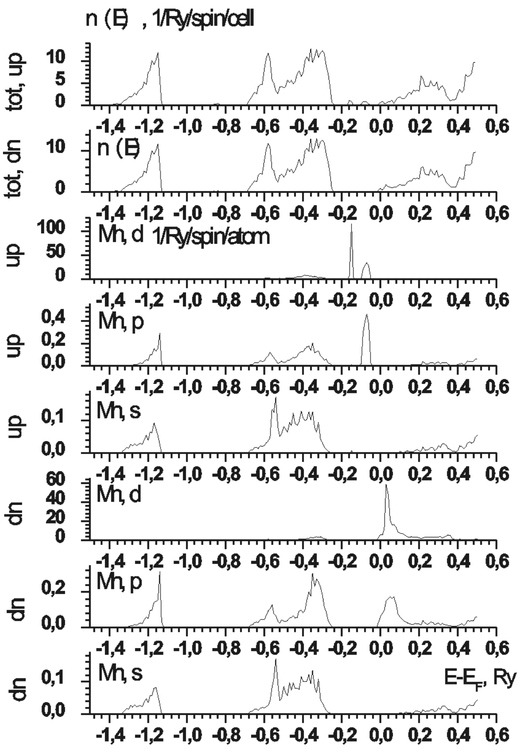

Fig. 8. The same as in Fig.1 for the Mn-doped (2%) AlN crystal co-doped with P (1%)

the influence of B, Si, and P impurities. One observes a considerable rise of the Fermi energy caused by Si and P impurities, whereas the B impurity isovalent with Al, on the contrary, results in a somewhat lowering of the Fermi level. The partial electron state densities shown in Figs. 1 and 2 are almost identical in the form and the localization. One can see that the partial densities of up-spin Mn states with p- and d-symmetry are localized at the Fermi level, while the densities of unoccupied down-spin Mn states with p- and d-symmetry are located above the Fermi energy.

In Figs. 3–4, one observes the variation of the curves of the partial electron state densities induced by Si and P impurities. The partial density curves of down-spin Mn states with p- and d-symmetry have shifted closer to the Fermi level, while the corresponding curves for up-spin states are now located below it. As follows from Table, the Si and P substitutional impurities lead to the growth of the magnetic moment on Mn.

Let us now analyze the calculation results obtained for the $\mathrm{Al_{0.98}Mn_{0.02}N}$, $\mathrm{Al_{0.97}Mn_{0.02}B_{0.01}N}$, and $\mathrm{Al_{0.97}Mn_{0.02}Si_{0.01}N}$ crystals. One can see from Table that the magnetic moment is absent even on the Mn atom, which qualitatively agrees with the experimental results reported in [8], where the paramagnetic behavior of $\mathrm{Al}_{1-x}\mathrm{Mn}_x\mathrm{N}$ films with concentrations $x = 0.05 - 0.10$ was revealed in the temperature range 10–300 K. In addition, one can see from Table that the Fermi energies and the electron state densities at the Fermi level are equal for different spin orientations. Figures 5 and 6 also demonstrate a complete identity of the partial density curves for the s-, p-, and d-symmetry states of Mn, which is an evidence of the paramagnetic state of the crystal.

However, the situation cardinally changes in the case of the $\mathrm{Al_{0.975}Mn_{0.02}P_{0.005}N}$ and $\mathrm{Al_{0.97}Mn_{0.02}P_{0.01}N}$ crystals. As follows from Table, the Fermi energies and the electron state densities at the Fermi level are different for the opposite spin orientations. So are the electron state densities presented in Figs. 7 and 8. The down-spin Mn states enter the conduction band, whereas the up-spin ones are located in the forbidden band in a vicinity of the Fermi level.

Thus, the B and Si substitutional impurities do not favor the ferromagnetic ordering in aluminum nitride with a 2-% manganese impurity, whereas the phosphorus impurity induces the appearance of the magnetic moment. At such a concentration of Mn atoms, the magnetic interaction between them is weak, while the wave functions of B and Si valence electrons are spatially localized. That is why, at low Mn concentrations (1%), B and Si atoms cannot initiate the superexchange mechanism. The increase of the Mn concentration to 2% in the presence of B and Si impurities also does not result in the required magnetism. However, P impurities at concentrations of 0.5% and 1% favor the maintenance of the magnetic ordering, which is well seen from Figs. 4, 7, and 8 and Table. The wave functions of P valence electrons are sufficiently delocalized in space to provide the magnetic interaction between manganese atoms even at low concentrations of both impurities.

4. Conclusions

B, Si, and P atoms belong to groups III, IV, and V, respectively. At low Mn concentrations, the $\mathrm{Al}_{1-x}\mathrm{Mn}_x\mathrm{N}$ ($x = 0.02$) crystal does not manifest magnetic properties. The Al→B substitution evidently cannot result in the appearance of the magnetism. Moreover, it leads to the lowering of the Fermi level. The Al→Si substitution also does not result in the magnetism, though, in this case, the number of valence electrons grows, which induces a rise of the Fermi level. The phosphorus doping raises the Fermi level because the number of valence electrons still grows. In addition, as one can see from Table, there appears a large magnetic moment on Mn atoms. Thus, the joint doping of aluminum nitride with atoms of $3d$ transition elements and nonmagnetic impurities can lead to the appearance or increase of the magnetic moment absent without an additional doping element.

The authors thank Prof. H. Akai (Osaka University) for the latest version of the KKR-LSDA-CPA (coherent potential approximation) software granted for calculations.

1. V.A. Dinh, K. Sato, and H. Katayama-Yoshida, J. of Superconduct. **18**, 47 (2005).
2. V.A. Dinh and H. Katayama-Yoshida, J. Elec. Micro. **54**, i61 (2005).
3. J. Kaczkowski and A. Jezierski, Acta Phys. Pol. A **115**, 275 (2009).
4. J. Korringa, Physica **13**, 392 (1947).
5. W. Kohn and N. Rostoker, Phys. Rev. **94**, 1111 (1954).
6. H. Akai and P.H. Dederichs, Phys. Rev. **B47**, 8739 (1993).
7. H. Akai, Phys. Rev. Lett. **81**, 3002 (1998).
8. T. Sato, Y. Endo, Y. Kawamura, F. Kirino, R. Nakatani, and M. Yamamoto, IEEE Trans. on Magnetics, **44**, 2688 (2008).

Received 09.11.10.
Translated from Ukrainian by H.G. Kalyuzhna

ВПЛИВ ЛЕГУВАННЯ АТОМАМИ B, Si ТА P НА ЕЛЕКТРОННІ ВЛАСТИВОСТІ КРИСТАЛА AlN З ДОМІШКОЮ Mn

С.В. Сиротюк, В.М. Швед

Резюме

Розраховано парціальні й повні густини електронних станів кристала AlN з домішкою Mn, додатково легованого атомами B, Si та P, для орієнтацій спінового моменту вниз і вгору. Порівняння густин електронних станів чистого і легованого Mn кристала AlN показує, що завдяки домішці Mn у забороненій зоні з'являються гібридизовані енергетичні стани *p*- і *d*-симетрії. Додаткове легування атомами B, Si та P спричиняє зміну густини електронних станів та значень спінових магнітних моментів на всіх атомах кристала.